Supporting materials for

Relationships between the planetary boundary layer height and surface pollutants derived from lidar observations over China

Tianning Su[1], Zhanqing Li[1,2*], Ralph Kahn[3]

[1]Department of Atmospheric and Oceanic Sciences & ESSIC, University of Maryland, College Park, M aryland 20740, USA

[2]State Key Laboratory of Earth Surface Processes and Resource Ecology and College of Global Change and Earth System Science, Beijing Normal University, 100875, Beijing, China

[3]Climate and Radiation Laboratory, Earth Science Division, NASA Goddard Space Flight Center, Greenbelt, MD, USA

* *Correspondence to:* Zhanqing Li (zli@atmos.umd.edu)

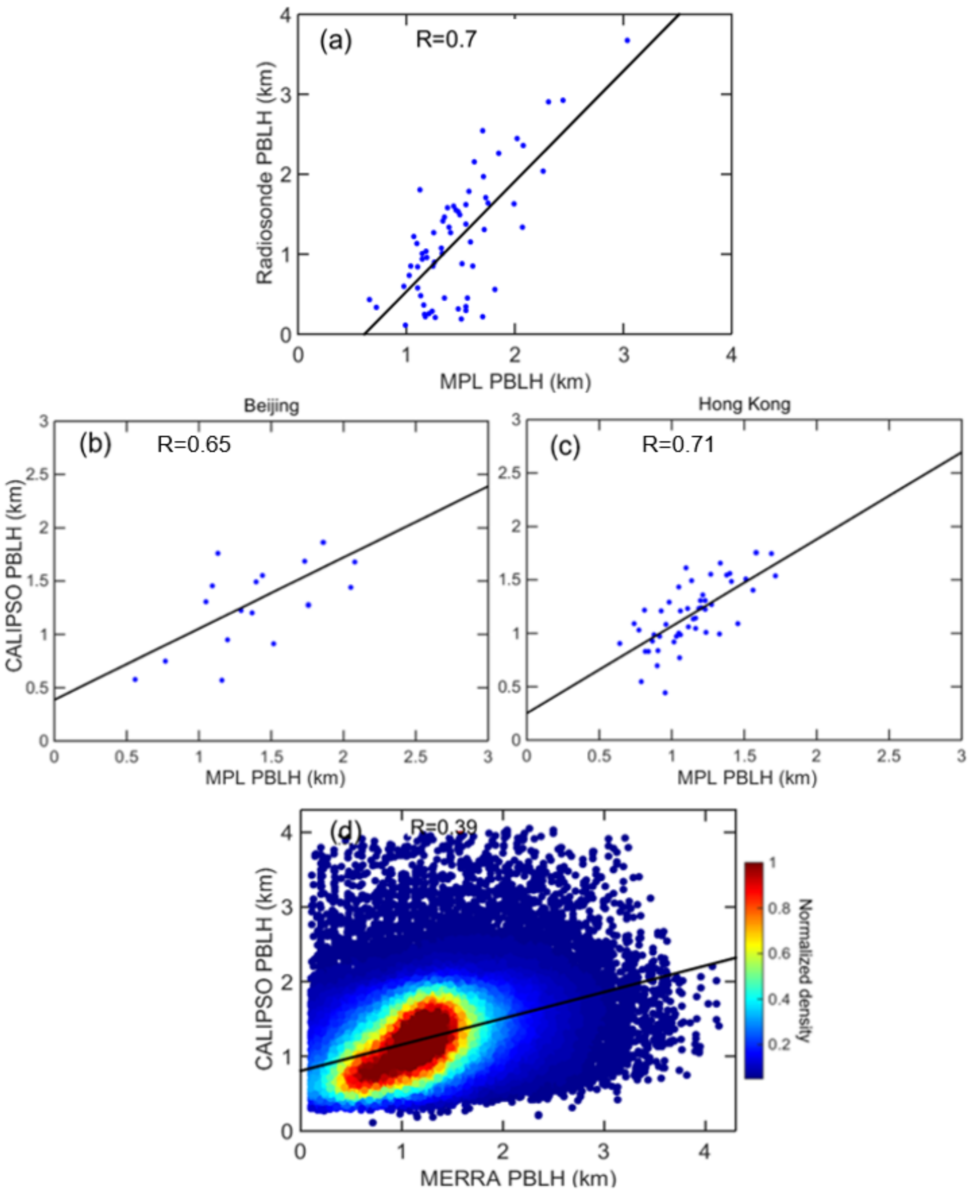

Figure S1. (a) The comparison of noontime PBLHs derived from MPL and radiosonde at Beijing. (b) The comparison of noontime PBLHs derived from CALIPSO and MPL at Beijing. (c) The comparison of noontime PBLHs derived from CALIPSO and MPL at Hong Kong. This comparison is adapted from Su et al. (2017). (d) The comparison of noontime PBLHs derived from CALIPSO and MERRA.

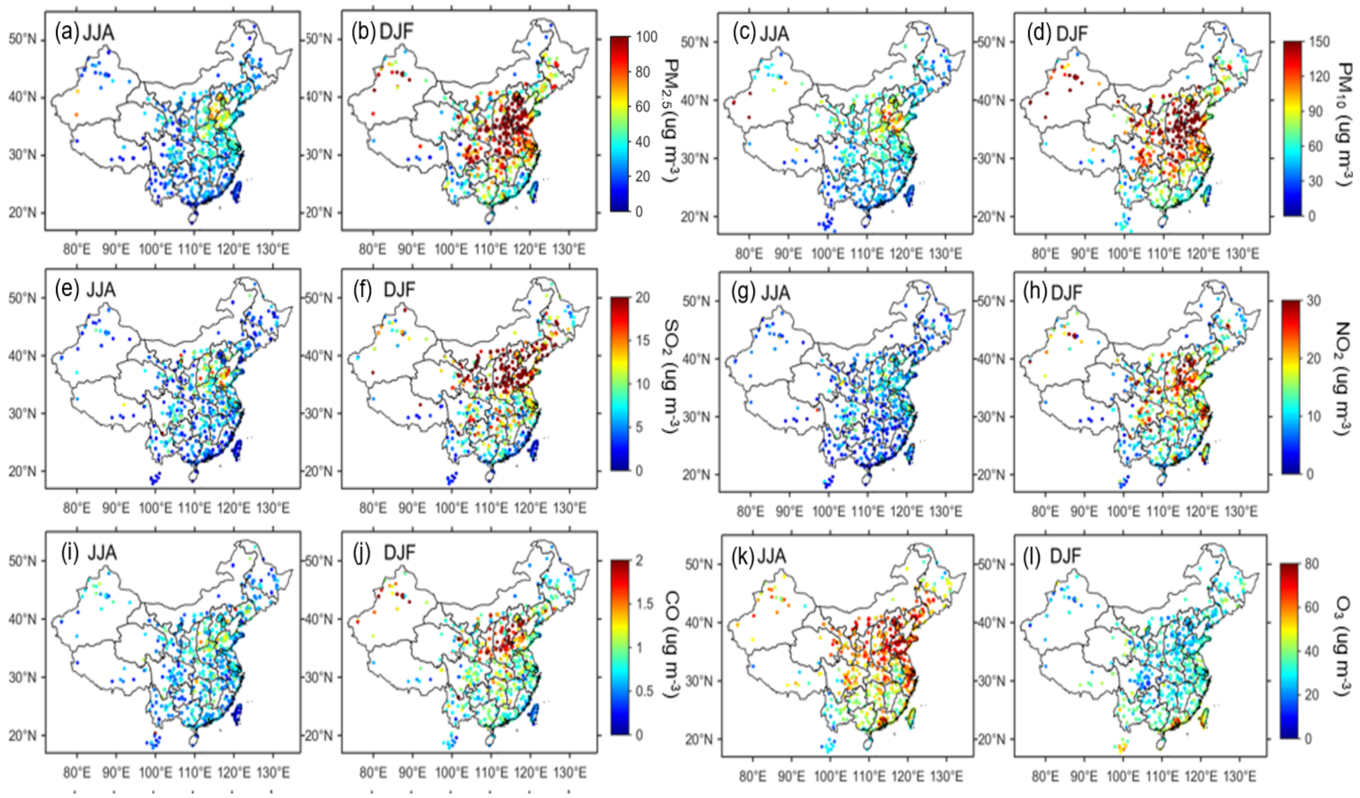

Figure S2. Spatial distributions of climatological $PM_{2.5}$ for (a) JJA and (b) DJF during the period 2012–2017. Spatial distributions of climatological PM_{10} for (c) JJA and (d) DJF. Spatial distributions of climatological SO_2 for (e) JJA and (f) DJF. Spatial distributions of climatological NO_2 for (g) JJA and (h) DJF. Spatial distributions of climatological CO for (i) JJA and (j) DJF. Spatial distributions of climatological O_3 for (k) JJA and (l) DJF.

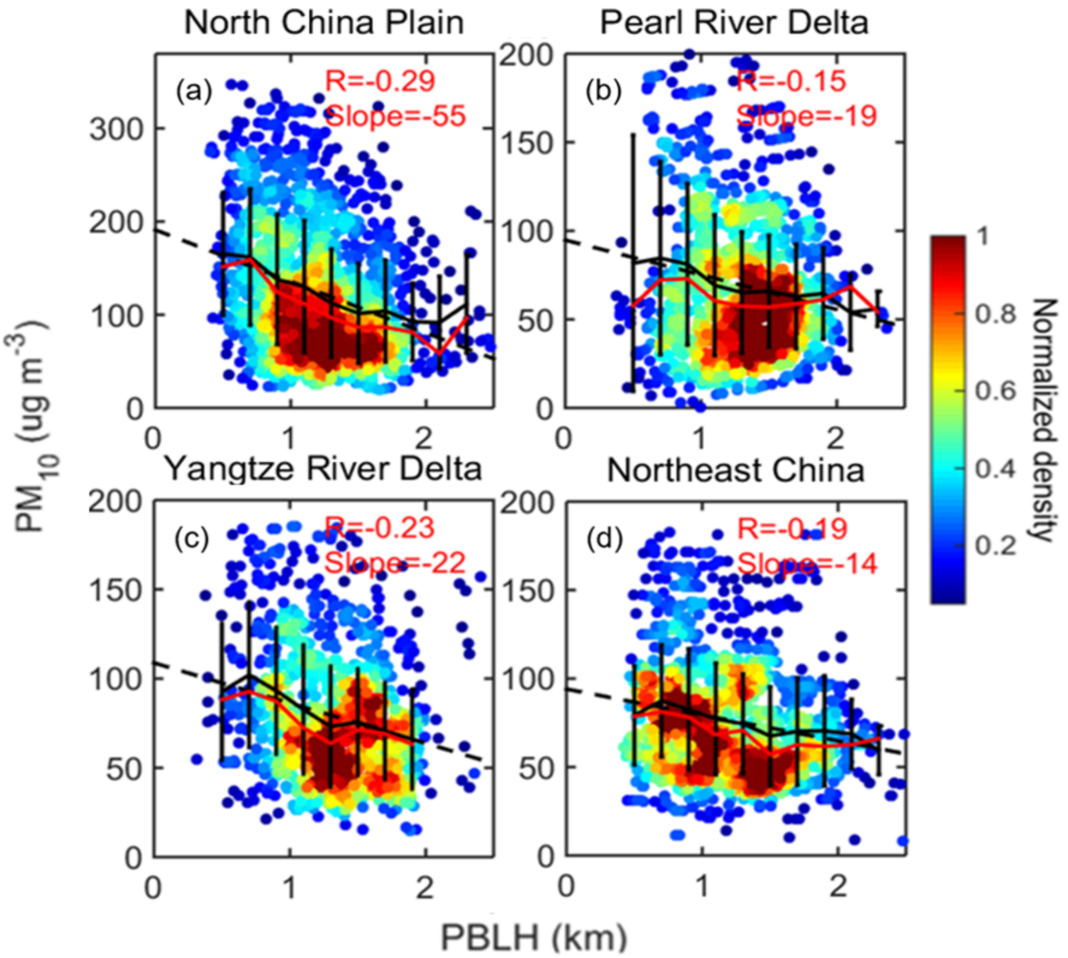

Figure S3. The relationship between PBLH and noontime PM_{10} over (a) NCP, (b) PRD, (c) YRD, and (d) NEC.

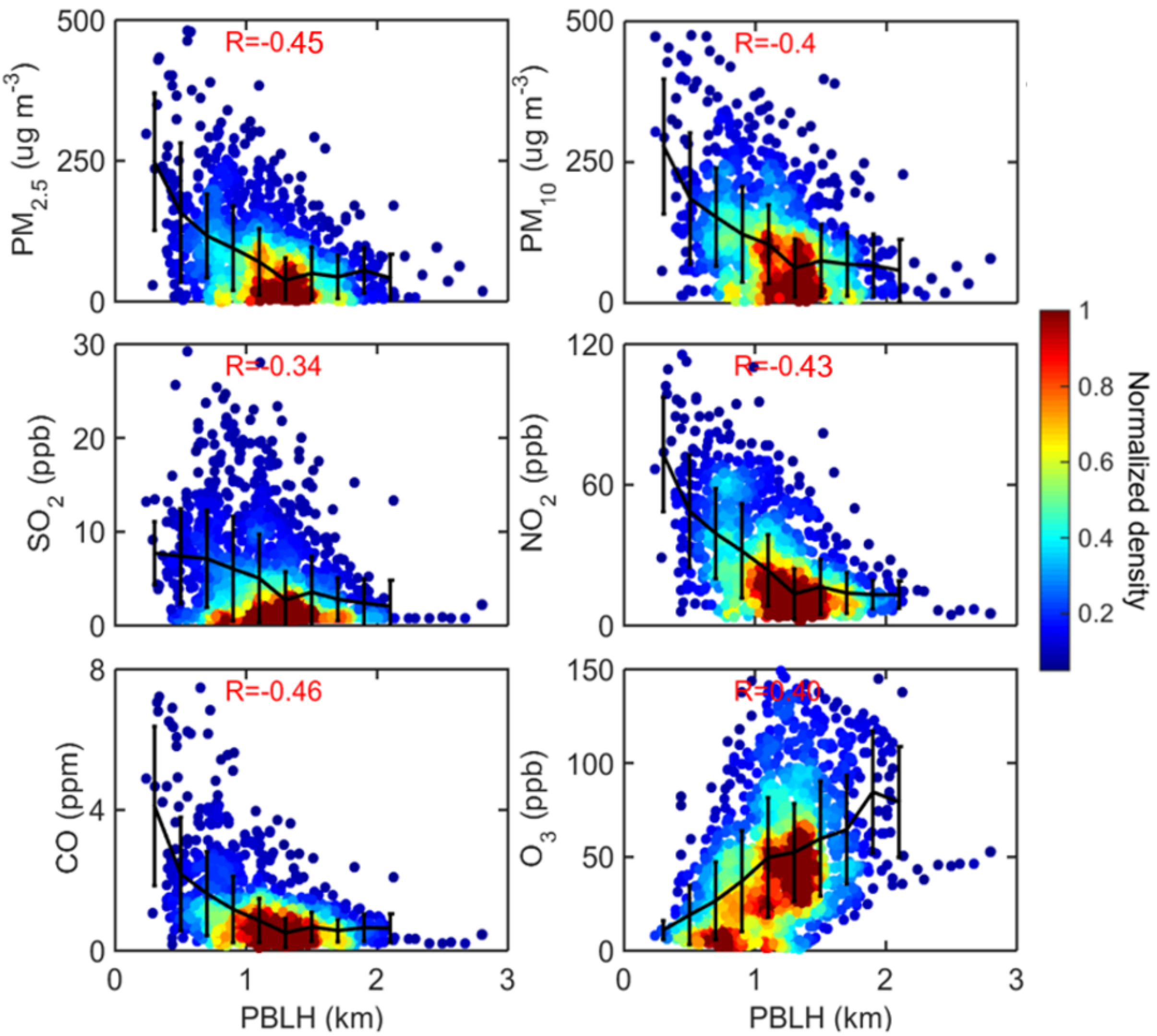

Figure S4. Relationships between MPL-derived PBLH and $PM_{2.5}$/PM_{10}/SO_2/NO_2/CO/O_3 over Beijing. Correlation coefficients (R) are shown in red in each panel. We use only data acquired during 1000–1500 local time, when the PBL is well developed. The relationships between CALIPSO-derived PBLH and PM/SO_2/NO_2/CO (presented in Figure 3 and Figure 10) are similar to the results derived from MPLs, including the unique PBLH-O_3 relationship.

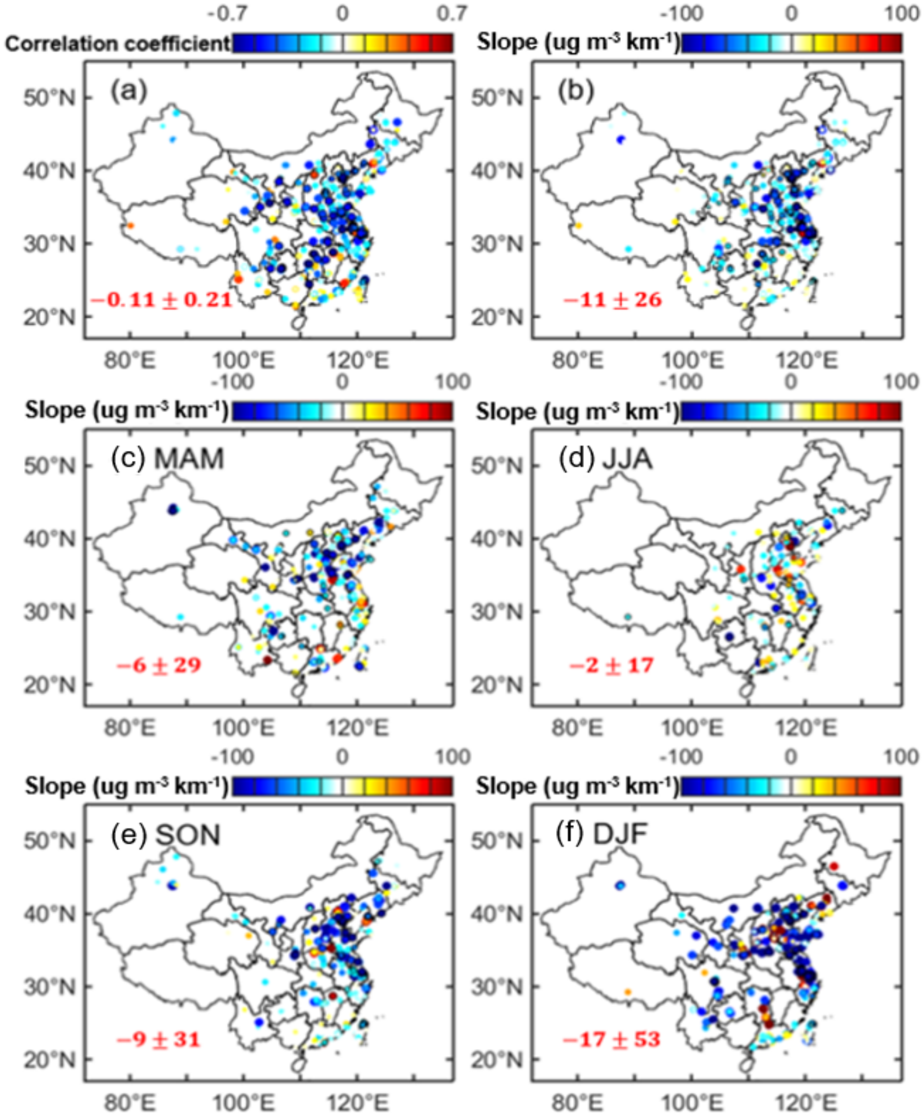

Figure S5. Spatial distributions of (a) correlation coefficients and (b) slopes (unit: μg m^{-3} km^{-1}) of the relationship between CALIPSO PBLH and $PM_{2.5}$. Spatial distributions of the slopes of the PBLH-$PM_{2.5}$ relationships for (c) MAM, (d) JJA, (e) SON, and (f) DJF. Dots marked with black circles indicate where the relationship between $PM_{2.5}$ and PBLH is statistically significant at the 95% confidence level. Mean values and standard deviations are shown in red at the bottom of each panel.

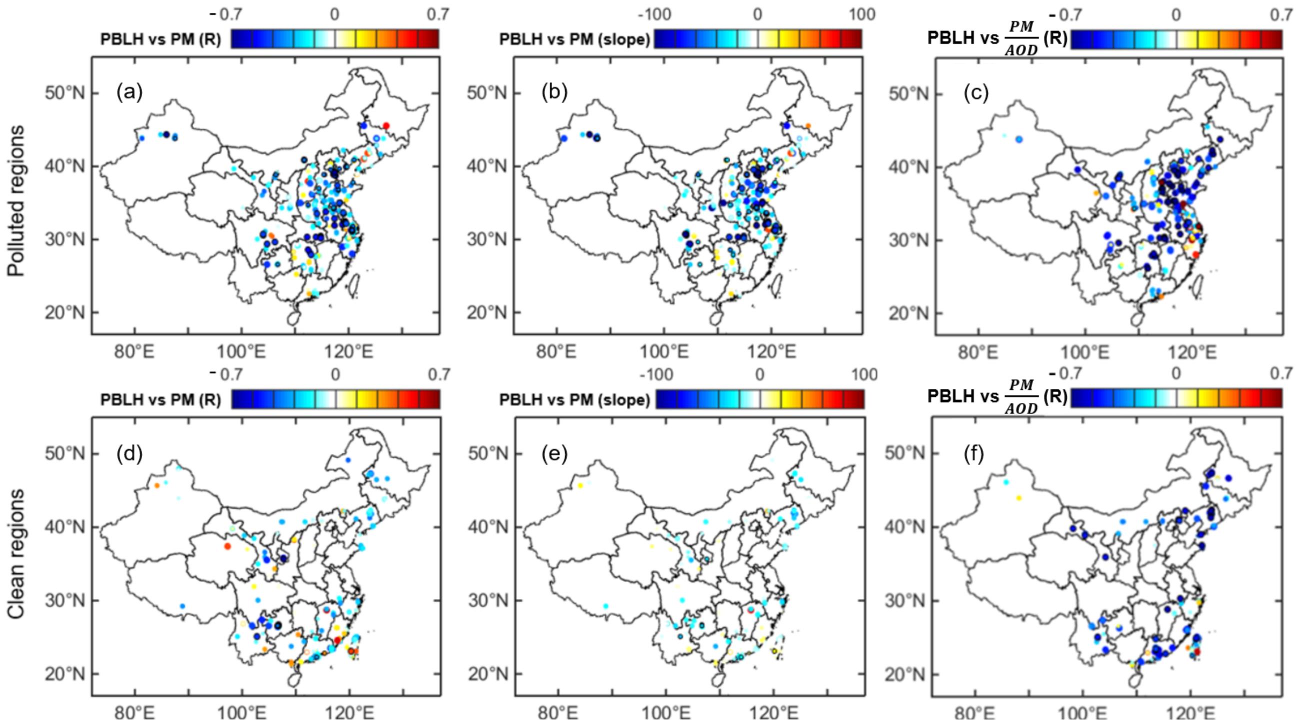

Figure S6. Stratification by annual pollution levels. The correlation coefficients (R) and slopes between PBLH and noontime $PM_{2.5}$ for polluted regions (a-b) (annual mean $PM_{2.5}$>40 ug m^{-3}) and clean regions (d-e) (annual mean $PM_{2.5}$<40 ug m^{-3}). The correlation coefficients (R) between PBLH and $PM_{2.5}$/AOD for polluted regions (c) and clean regions (f). Noted the PBLH-PM correlations are much stronger for polluted regions. After normalizing $PM_{2.5}$ by AOD, the correlations are much stronger for most stations, especially for those over clean region.

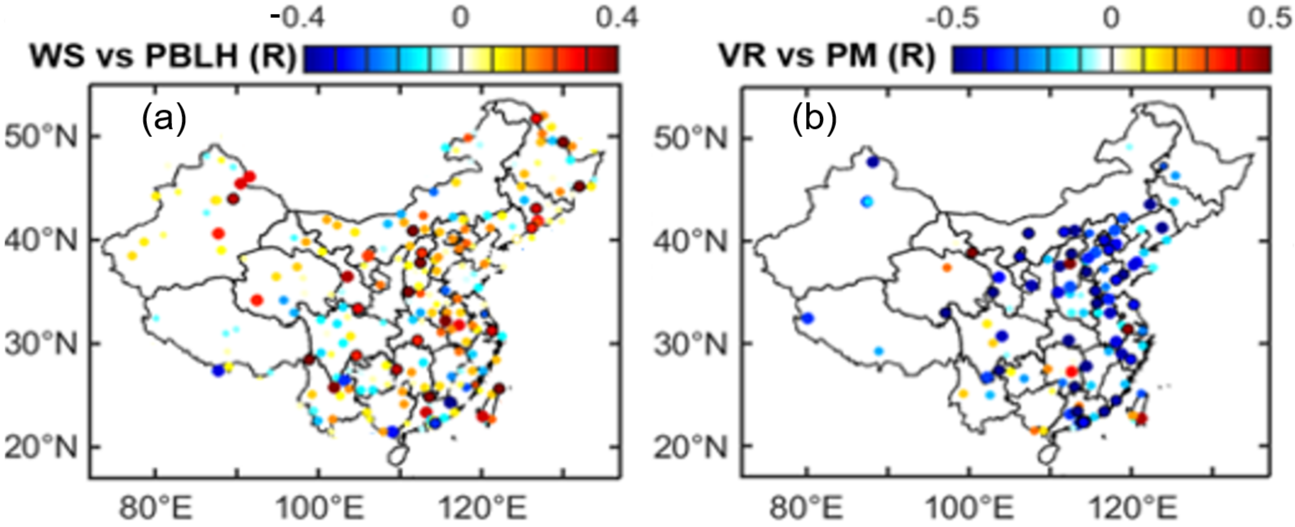

Figure S7. (a) Spatial distribution of correlation coefficients (R) for the WS-PBLH relationship. (b) Spatial distribution of correlation coefficients (R) for the VR-$PM_{2.5}$ relationship.

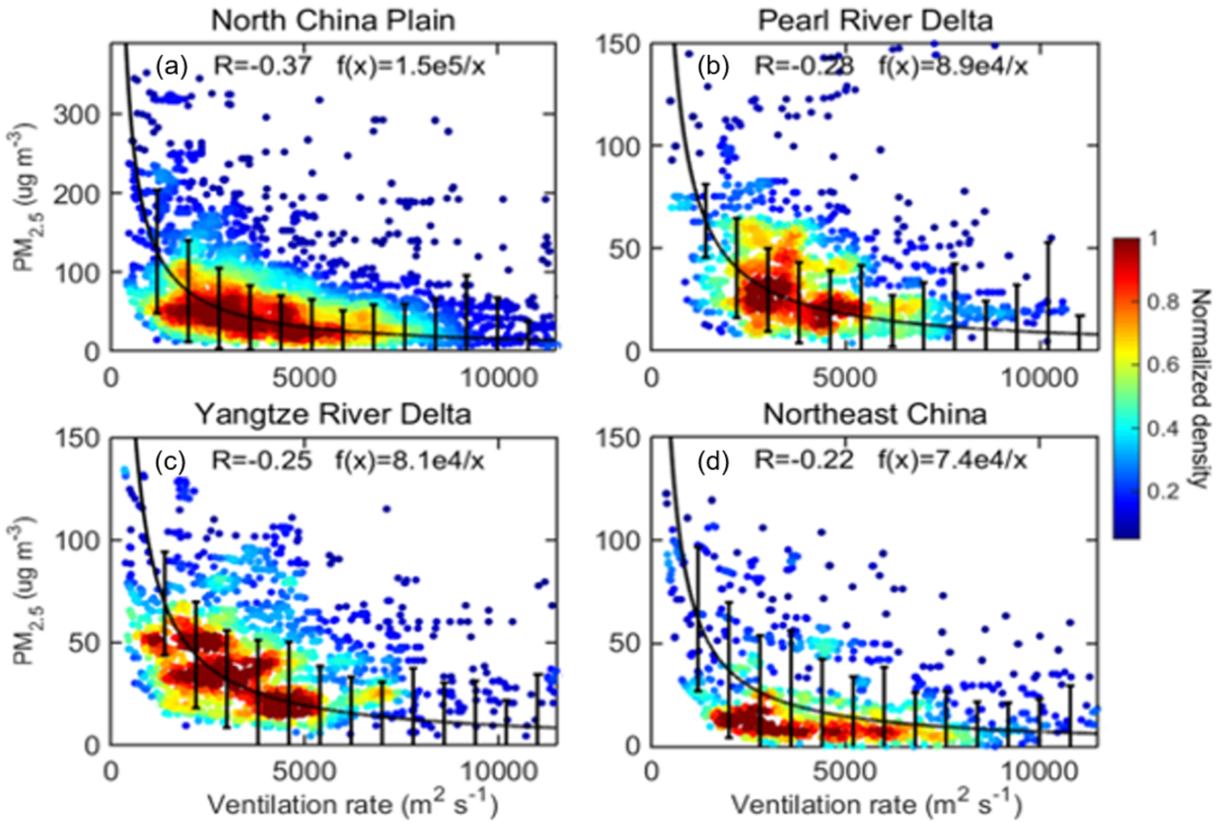

Figure S8. The relationship between noontime $PM_{2.5}$ and ventilation rat over (a) the NCP, (b) PRD, (c) YRD, and (d) NEC.

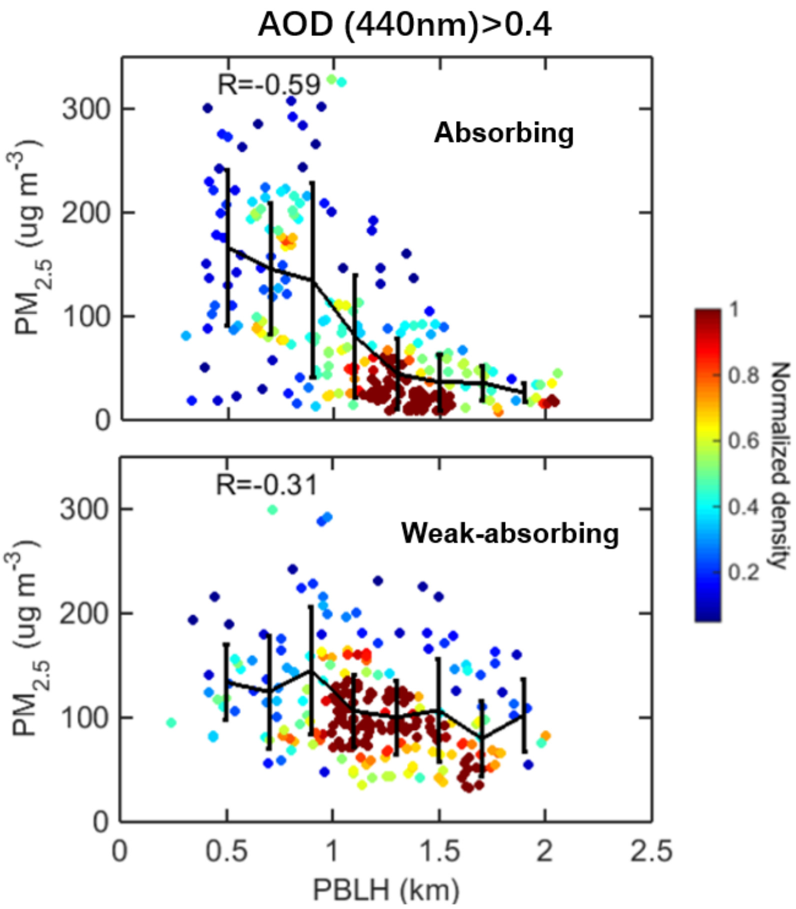

Figure S9. The relationship between hourly $PM_{2.5}$ and PBLH for (a) absorbing aerosols and (b) weak-absorbing over Beijing. We only selected the cases when AOD at 440nm is above 0.4.

References

Su, T., Li, J., Li, C., Xiang, P., Lau, A.K.H., Guo, J., Yang, D. and Miao, Y.: An intercomparison of long- term planetary boundary layer heights retrieved from CALIPSO, ground- based lidar, and radiosonde measurements over Hong Kong. Journal of Geophysical Research: Atmospheres, 122(7), pp.3929-3943, 2017.